Electrochemical Generation of Porphyrin-Porphyrin and Porphyrin-C$_{60}$ Polymeric Photoactive Organic Heterojunctions

María Belén Suarez [a], Javier Durantini [a], Luis Otero [a,*], Thomas Dittrich [b], Marisa Santo [c], María Elisa Milanesio [a], Edgardo Durantini [a], Miguel Gervaldo [a,*]

[a] Departamento de Química, Universidad Nacional de Río Cuarto, Agencia Postal Nro. 3, X5804BYA Río Cuarto, Córdoba, Argentina
[b] Helmholtz Center Berlin for Materials and Energy, Institute of Heterogeneous Materials, Hahn-Meitner-Platz 1, D-14109 Berlin, Germany
[c] Departamento de Física, Universidad Nacional de Río Cuarto, Agencia Postal Nro. 3, X5804BYA Río Cuarto, Córdoba, Argentina

ARTICLE INFO

ABSTRACT

Photoactive organic-organic interfaces are formed by electrochemical synthesis. The generation of porphyrin/porphyrin and porphyrin/C$_{60}$ heterojunctions over indium tin oxide electrodes by successive electropolymerization steps is described. Functionalized C$_{60}$ buckminsterfullerene holding a carbazol residue and porphyrins containing carbazol and phenylamino moieties are able to form electrodeposited layers by cyclic voltammetry. Photoinduced electron transfer between Zn(II), free base porphyrins and C$_{60}$ films were analyzed by both, light modulated surface photovoltage spectroscopy and laser induced transient photovoltage. The results showed that the electrochemical generated polymeric heterojunctions are able to produce photoinduced charge separated states, which could present a potential application in the design and construction of organic optoelectronic devices.

© 2014 Elsevier Ltd. All rights reserved.

1. Introduction

The development of organic materials with application in optoelectronic devices, like organic solar cells and organic light emitting diodes, have shown a remarkable scientific activity due to the relevance of these technologies in the generation and rational use of energy [1]. The application of organic materials in optoelectronics is a challenging target, because these materials must be designed in order to include efficient light absorption and/or emission capability, adequate electron work function, appropriate electron and hole transport, malleability, suitable solid properties and chemical stability.

Essentially, organic-based optoelectronic devices utilize heterogeneous junction regions that dissociate excitons to produce separated electrical charges. These heterojunction regions may be bulk-heterojunctions or boundaries formed by an electron donor layer and an electron acceptor layer. Devices formed by combining conducting polymers (as electron donor and hole-transport layers) and fullerenes (as electron acceptor and electron-transport) have demonstrated to produce high efficiency in the conversion of solar radiation into electrical energy [2] and are promising to be used in new solar energy technologies. However, the employment of organic materials in the development of optoelectronic devices involves the formation, characterization and application of supramolecular arrangements, polymeric and oligomeric structures for application in thin films. Thus, the control of molecular assembly to generate organized architectures is an important factor in this field. The most used methods to deposit organic materials for optoelectronic devices assemblage are thermal evaporation and solution-processing (drop casting, spin coating, etc). Although thermal evaporation produces well-patterned films, the process is slow and demands an expensive vacuum equipment. In addition, thermal evaporation requires materials with high sublimation capability and excellent thermal stability, which are properties that are not easily obtained in polymers. Also, low-cost solution processes, such as spin-coating, and deep-coating require materials with intrinsic high solubility, and usually produce a large amount of waste. An important alternative technique to produce organic heterojunctions is electropolymerization. The deposition of organic materials over a conducting substrate through electrochemical polymerization is a versatile method that allows synthesizing a conducting film in one step [3–7].This deposition method has been used in the formation of donor-acceptor heterojunctions which were successfully employed in solar cells. Nasybulin et al. have designed a herojunction solar cell by successive

* Corresponding authors. Tel.: +54-(0)358-4676195; fax: +54-(0)358-4676233.
E-mail addresses: mgervaldo@exa.unrc.edu.ar, miguel.gervaldo@hotmail.com (M. Gervaldo).

electropolymerization of the donor and acceptor layers [8],and an interesting bulk herojunction solar cell by electrochemical codeposition of the donor-acceptor materials [9].

Due to their unique electronic, magnetic and optical properties, many studies on the development of optoelectronic devices incorporate porphyrins, chlorophyll derivatives, and several related metallized and unmetallized tetrapyrrolic compounds [10–16]. The electrochemical oxidation-induced polymerization of porphyrins containing aniline, phenol, pyrrole, vinyl and thiophene substituents has been extensively researched for many years [17–20] and, in general, this method allows the production of homogeneous electroactive thin films. Recently we reported the synthesis, characterization and electrochemical polymerization of porphyrin derivatives with two different functionalities; carbazol (CBZ) and triphenylamine (TPA) configured in a cross fashion as meso substituents. Films formed by dicarbazole (DCBZ) and tetraphenylbenzidine (TPB) (two well-known hole-transporting materials) electrochemically generated over a semi-transparent surface showed the production of photoinduced charge separation states and charge migration upon porphyrin excitation, making them promising candidates for application in optoelectronics devices [21].

In this work we describe the generation of porphyrin/ porphyrin and porphyrin/C_{60} photoactive heterojunctions by successive electropolymerization steps. 5,15-bis[4(-*N*,*N*-diphenyl-amino)phenyl]-10,20-bis[3-(*N*-ethylcarbazoyl)]porphyrin (**PCBZ-TPA**, denoted by **A** in Fig. 1a) and Zn(II) 5,15-bis [4(-*N*,*N*-diphenylamino)phenyl]-10,20-bis[3-(*N*-ethylcarbazoyl)] porphyrin (**PCBZTPA-Zn**, denoted by **B** in Fig. 1a) form photoactive electropolymerized bilayers over indium tin oxide (ITO) semitransparent electrodes. We also report the synthesis of a functionalized C_{60} buckminsterfullerene holding a carbazol residue (N-methyl-2-(9-ethyl-3-carbazoyl) fulleropyrrolidine), **C_{60}CBZ**, denoted by **C** in Fig. 1b) that forms electrodeposited layers by cyclic voltammetry (CV). The deposition of **C** over **B** and **A** polymeric films allows the formation of photoactive heterojunctions by a simple methodology. In an idealized system (Fig. 1c), it can be assumed that in the organic-heterojuntions polymer **B** acts as a donor in **ITO/A/B**, **ITO/B/A** and **ITO/B/C** bi-layer systems, and that polymer **A** acts as an acceptor in **ITO/A/B** and **ITO/B/A** layer systems, but as a donor in **ITO/A/C** bi-layers. Our assumption is based on the fact that Zn porphyrins act as electron donors while free base porphyrins act as electron acceptors in porphyrin-porphyrin dyad molecular systems [22–24]. On the other hand, it is well known that C_{60} is one of the best and most used acceptor molecules. Photoinduced charge separation states have been observed before in porphyrin/C_{60} systems, where the porphyrin acts as the donor unit, and the C_{60} as the acceptor [25].

The formation of photoinduced charge separation states in the films is demonstrated by surface photovoltage generation in both, modulated spectroscopy (Surface Photovoltage Spectroscopy, SPV) and laser induced transient photovoltage. The results show that the electrochemical generated polymeric heterojunctions are able to produce photoinduced charge separated states, which present potential application in the design and construction of optoelectronic devices.

2. Experimental

2.1. C_{60}CBZ monomer synthesis

A solution of C_{60} (60 mg, 0.083 mmol), 9-ethyl-3-carbazolecarbaldehyde (20 mg, 0.090 mmol) and N-methylglycine (8 mg, 0.090 mmol) in 60 mL of dry toluene was stirred at reflux in atmosphere of argon for 6 h. Then, the solvent was removed under vacuum and the solids purified by flash column

chromatography (silica gel) using toluene/cyclohexane (80:20) and pure toluene as eluent. After that, the solvents were evaporated under vacuum yielding 21 mg (26%) of N-methyl-2-(9-ethyl-3-carbazoyl)fulleropyrrolidine. TLC (silica gel, toluene) analysis Rf = 0.80. ^{1}HNMR (CDCl$_3$, TMS) δ [ppm] 1.45 (t, 3H), 2.87 (s, 3H, N-CH$_3$), 4.30-4.40 (m, 4H), 5.06 (d, 1H), 5.13 (s, 1H), 7.33-7.52 (m, 6H), 8.16 (d, 1H). ESI-MS [m/z] 971.1548 (M+H)+ (970.1470 calculated for $C_{77}H_{18}N_2$).

2.2. Instrumentation and Measurements

Absorption spectra were recorded at $25.0\pm0.5\,^\circ$C using 1 cm path length quartz cells on a Shimadzu UV-2401PC spectrometer. Proton nuclear magnetic resonance spectra were recorded on an FT-NMR Bruker Avance DPX400 spectrometer at 400 MHz. Mass Spectra were taken with a Bruker micrO-TOF-QII (Bruker Daltonics, MA, USA) equipment with an ESI source operated in positive/negative mode, using nitrogen as nebulizing.

The voltammetric characterization of the redox processes and electropolymerization deposition of the porphyrins was performed with a potentiostat-galvanostat Autolab (Electrochemical Instruments) in a conventional three-electrode cell. Two kinds of working electrodes were used: Pt and Indium tin oxide (ITO, Delta Technologies, nominal resistance 8–12 Ω/square). ITO electrodes were employed to form the bilayers used in SPV and UV-vis spectroscopy experiments. When large area ITO electrodes were used the counter electrode was isolated from the monomer solution by a glass frit in order to avoid interference with the redox reactions occurring at the working electrode. Electrochemical studies of porphyrins were carried out in 1,2-dichloroethane (DCE) deoxygenated solution (nitrogen bubbling), with 0.10 M tetra-*n*-butylammonium hexafluorophosphate (TBAPF$_6$) as the supporting electrolyte, and in o-dichlorobenzene (o-DCB) deoxygenated solution (nitrogen bubbling) for **C**, with 0.10 M tetra-*n*-butylammonium tetrafluoroborate as the supporting electrolyte. All the electrochemical responses of the electropolimerized films were carried out in (DCE) deoxygenated solution (nitrogen bubbling), with 0.10 M tetra-*n*-butylammonium hexafluorophosphate (TBAPF$_6$) as the supporting electrolyte. In all the electrochemical measurements a large area Pt counter electrode, and a silver wire quasi-reference electrode were used. After each voltammetric experiment, ferrocene was added as an internal standard, and the potential axis was calibrated against the formal potential for the Saturated Calomel Electrode (SCE). The Pt working electrode was cleaned between experiments by polishing with 0.3 μm alumina paste followed by solvent rinses.

The measurements of modulated Surface Photovoltage (SPV) were performed in the fixed capacitor arrangement with chopped light (modulation frequency 6 Hz) from a quartz prism monochromator (SPM2) and a halogen lamp (100 W) [26]. The SPV signals were detected with a high impedance buffer (measurement resistance 10 GΩ). The measurements were carried out in vacuum. The SPV spectra were not normalized to the photon flux, and the ITO electrodes were illuminated from the front side (porphyrin layer facing the light). The in-phase (equivalent to the sine) and phase-shifted by 90° (equivalent to the cosine) signals are measured with the two-phase lock-in amplifier (EG&G, model 5210). The phase shift has been calibrated with a Si photodiode. The sign of the in-phase SPV signal is positive (negative) if the photo-generated electrons are preferentially separated towards the internal (external) surface. The amplitude of the modulated SPV signal is defined as the square root of the sum of the squared in-phase and 90° phase-shifted SPV signals.

SPV transients were excited with laser pulses (wavelength 600 nm, time of laser pulses: 5 ns, intensity: about 3 mJ/cm^2) and recorded with a sampling oscilloscope (GAGE compuscope CS
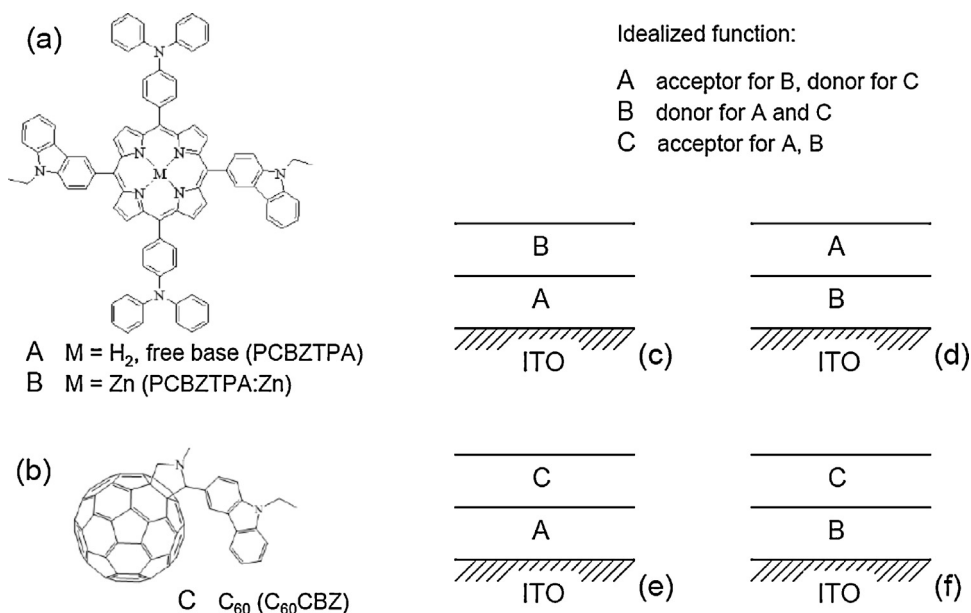
Idealized function:

A acceptor for B, donor for C
B donor for A and C
C acceptor for A, B

Fig. 1. Chemical structure of (a) **PCBZTPA** (denoted by **A**), **PCBZTPA-Zn** (denoted by **B**) and (b) **C₆₀-CBZ** (denoted by **C**) molecules and combinations of electrodeposited bi-layer systems (**ITO/A/B**, **ITO/B/A**, **ITO/A/C**, **ITO/B/C** – (c-f), respectively).

14200) at resolution of 10 ns. The ITO electrodes were illuminated from the front side (porphyrin layer facing the light).

3. Results and discussion

3.1. Electrochemical formation of B/A and A/B bilayers

To form the respective **B**/**A** and **A**/**B** bilayers, **A** and **B** were electropolymerized one on top of the other one in two different arrangements, using cyclic voltammetry. The first one consists of a layer of **B** on top of the Pt electrode and a second layer of **A** on top of the first one (**B**/**A**). The second configuration was formed the other way around (**A**/**B**). Fig. 2a and b show the first (black line) and the fifth (red line) anodic scans at a platinum electrode of **B** and **A** monomers, respectively. In both cases increases in the oxidation/reduction currents are detected after the five cycles. When the

electrodes are transferred to a DCE solution containing only support electrolyte they present bell shaped cyclic voltammograms (Fig. 3a and b, black lines), and the oxidation/reduction peak currents for these couples are proportional to the scan rate. This confirms the formation of a film on the electrodes (first layer). The second layer was also formed by electropolymerization, cycling a film of **B** in a **A** solution, and a film of **A** in a **B** solution. When the respective electrodes are cycled between 0 V and the most anodic oxidation peak for five cycles, they show increases in the oxidation/reduction currents (Fig. 2a and b blue lines). Also, after the electrodes are removed from the porphyrin solutions and placed in a solution free of monomer they present redox couples at similar potentials than those observed after polymerization of the first layer. It can be seen from Fig. 3a and b that the peak currents for the new redox systems are increased after the formation of the second layer (red lines), confirming the formation of the bilayers on the electrode surface.
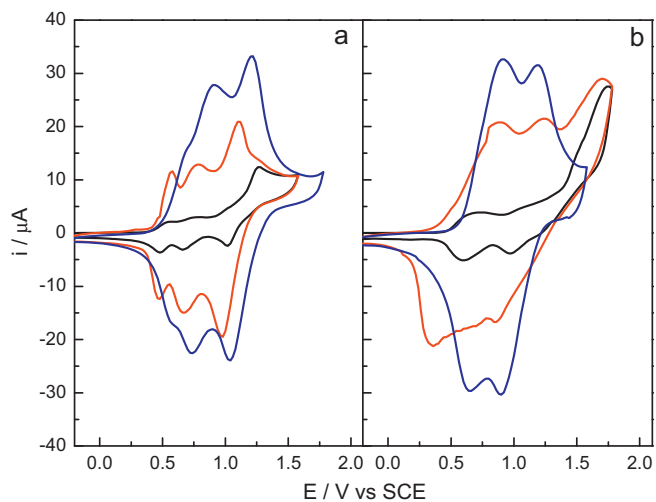

Fig. 2. (a) First (black) and fifth (red) cyclic voltammogram of **B**, and fifth (blue) cyclic voltammogram of **A** monomers, obtained during formation of the **B/A** bilayer. (b) First (black) and fifth (red) cyclic voltammogram of **A**, and fifth (blue) cyclic voltammogram of **B** monomers, obtained during formation of the **A/B** bilayer. All measurements were done in DCE containing TBAPF₆ using a Pt working electrode.
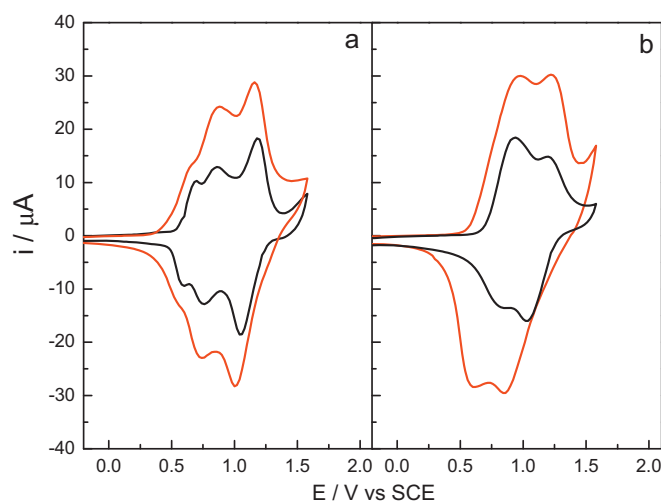

Fig. 3. Electrochemical responses of electropolymerized films of (a) **B/A**, and (b) **A/B**, in DCE containing only support electrolyte. Black lines after deposition of the first layer and red lines after deposition of the second layer. Pt working electrode. Scan rate: 100 mV/s.
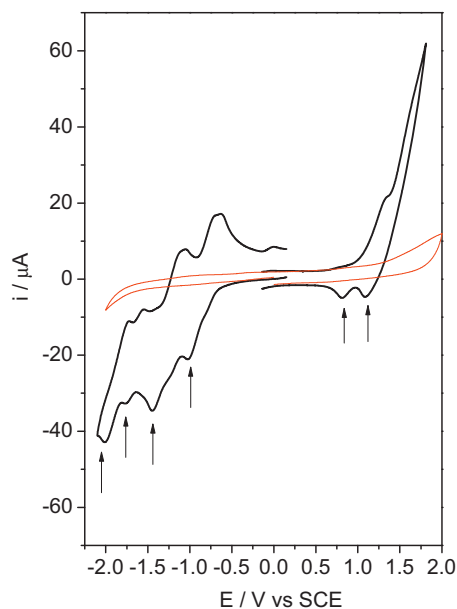
Fig. 4. First anodic and cathodic scans of **C**, in o-DCB containing TBAPF$_6$ using a Pt working electrode (black line), and solvent/electrolyte blank (red line). Scan rate: 100 mV/s.
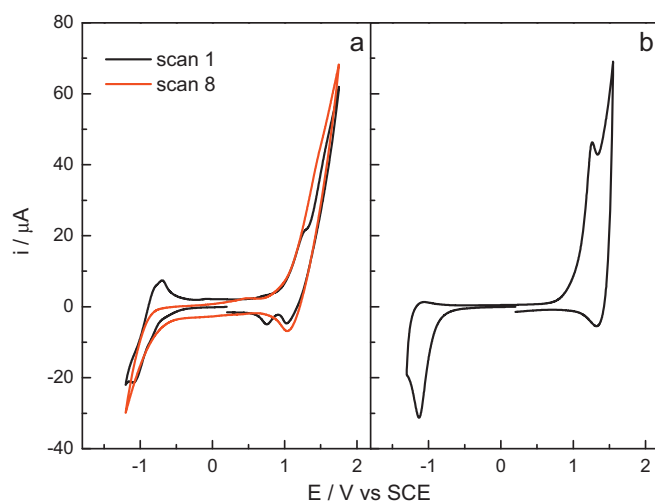

Fig. 5. (a) First and eighth cyclic voltammograms of **C** in o-DCB containing TBAPF$_6$ using a Pt working electrode. (b) Cyclic voltammogram of a electrodeposited film of **C** in DCE containing TBAPF$_6$ using a Pt working electrode. Scan rates: 100 mV/s.

The electrochemical properties of **B**, **A**, and their electropolymerizations on different substrates have been previously reported [21]. Based on electrochemical and spectroelectrochemical studies, polymer structures in which the porphyrin units are linked by TPB and DCBZ groups were proposed. Therefore, formation of the bilayers may occur in a similar way. Possibly, some free TPA and CBZ groups that did not react during the formation of the first layer could react with TPA and CBZ groups arriving from the other porphyrin solution used in the formation of the second layer. Also, the subsequent layer could be formed just by dimerization of TPA and CBZ groups present in the porphyrin used in the second electropolymerization procedure.

The bilayer formations were also carried out on ITO electrodes. After deposition of the layers the absorption spectra showed bands which correlate with the absorption spectra of the free base and Zn derivative monomers in solution (see UV-Visible Absorption properties for more details).

3.2. Electrochemical formation and characterization of A/C and B/C bilayers

Fig. 4 shows the first catodic and anodic scan of **C** in o-DCB solution containing TBAPF$_6$. Four reversible reduction peaks are observed at -0.81, -1.25, -1.66, and -1.88 V, which are assigned to reduction of the C$_{60}$ unit [27,28]. In the anodic direction an irreversible oxidation peak appears at about 1.34 V, and an increasing anodic current is inferred at 1.63 V, which is superimposed with the onset of the solvent/electrolyte decomposition. Also in the backward scan two small peaks (denoted by arrows) appear at 1.08 and 0.82 V, which could be indicative of a chemical reaction coupled to the electron transfer. Repetitive cycling of **C** between -1.20 and 1.75 V, produces a small increase in the oxidation/reduction currents after each scan (Fig. 5a), typical of a product irreversibly absorbed on the electrode surface. Although the film is also formed by cycling in the anodic range (between 0.00 and 1.75 V), the electropolymerization showed in Fig. 5 was carried out between -1.20 and 1.75 V, to show that electrochemical processes related to C$_{60}$ reduction are present during and after polymerization. When the electrode was removed from the C solution and placed in DCE

solution containing only support electrolyte it showed two oxidation processes at 1.26 and 1.47 V (Fig. 5b), and one reduction peak at -1.13 V, confirming that an electroactive product has been adsorbed on the electrode.

The observed electrochemical behavior could be explained taking into account that **C** has one carbazole unit attached to the C$_{60}$ group through the 3 position. The two oxidation processes at 1.34 and 1.63 V in Fig. 4 could be assigned to the oxidation of the carbazole and C$_{60}$ moieties [29,30], and the two small reduction peaks could be related to the reduction of the DCBZ, generated during the forward scan [29,31]. It is known that oxidation of CBZ leads to dimerization of two radical cations through the 3,3' positions [29,31]. **C** has just a 3 position free, and probably dimers of **C** are formed during oxidation, which are absorbed on the electrode surface. Although it has been reported oxidative polymerization of C$_{60}$, in our experimental conditions, it must be discarded because previous studies demonstrated that nucleophilic counteranions such as PF$_6^-$, reacts with fullerene radical cations [32].

On the other hand, **B**/**C** and **A**/**C** bilayers were done electrodepositing a first layer of porphyrin and a second one of **C**. Fig. 6a and b show the first (black line) and fifth (red line) CV of **B** and **A** solutions, respectively, using a Pt electrode. Similar to the results observed in porphyrin/porphyrin bilayer formations, the oxidation/reduction currents are increased after five cycles, and the electrochemical responses of the electrodes observed in DCE solution containing only support electrolyte are showed in Fig. 7 (black lines). The **C** layer was deposited cycling the electrodes between -1.25 and 1.75 V, and the eighth cycles are shown in Fig. 6 (blue lines). In order to confirm the adsorption of **C** on the porphyrin layers, their electrochemical responses were carried out in DCE free of **C** (Fig. 7, red lines). The CVs show the generation of currents associated to oxidation of the porphyrin film, and on top of these the electrochemical processes related to **C**. Also, the currents are increased respect to those observed for the first porphyrin layer, indicating that more electroactive species are absorbed on the electrode The CVs present a reduction peak, which was not present after deposition of the porphyrin layers, therefore they must correspond to reduction of the **C$_{60}$** units.

Deposition of the **C** layer on top of the porphyrin layers could proceed by two ways. The first one may be the mechanism of dimerization of two **C** radical cations mentioned before, and the second one could probably be more complex, involving dimerization of
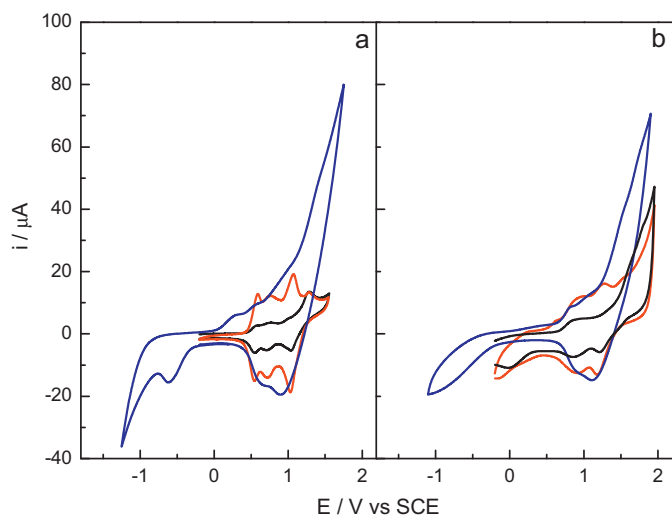
Fig. 6. (a) First (black) and fifth (red) cyclic voltammogram of **B** (in DCE), and eighth (blue) cyclic voltammogram of **C** monomer (in o-DBZ), obtained during formation of the **B/C** bilayer. (b) First (black) and fifth (red) cyclic voltammogram of **A** (in DCE), and eighth (blue) cyclic voltammogram of **C** monomer (in o-DBZ), obtained during formation of the **A/C** bilayer. All measurement were done using a Pt working electrode.

some free CBZ units present in the porphyrin layer with the CBZ units in the **C** solution, and/or both at the same time.

3.3. UV-Visible Absorption properties of A/B, and B/A electropolymerized bilayers

The electropolymerization of the bilayers was also confirmed by UV-vis spectroscopy. Fig. 8a shows representative absorption spectra of **ITO/A/B** bilayers. After deposition of the first layer the spectrum presents the Soret band, and the typical four Q bands due to the electronic transitions of **A** polymer (Fig. 8a red line). Electropolymerization of a second layer of **B** produces an enlargement in the absorbance of the bilayer. The increase in absorbance at 560 and 620 nm must be remarked. These two absorption bands, which are characteristic of the Zn layer, can be seen in the inset of Fig. 8a black line. As a result, the absorption spectrum is similar to a
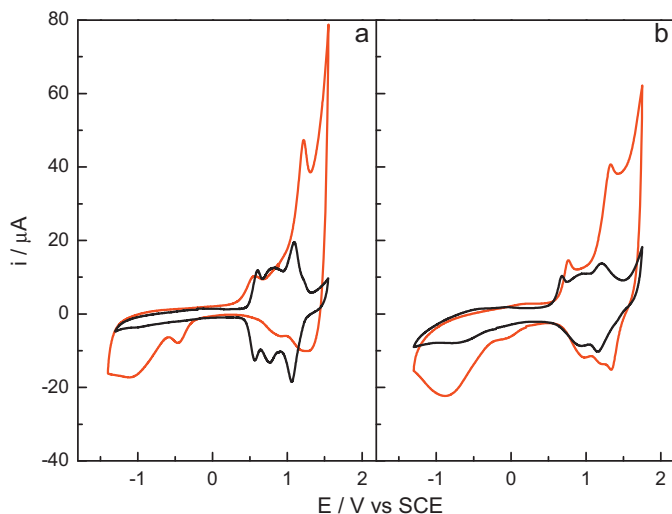

Fig. 7. Electrochemical responses of electropolymerized films of (a) **B/C**, and (b) **A/C**, in DCE containing only support electrolyte. Black lines after deposition of the first layer and red lines after deposition of the second layer. Pt working electrode. Scan rate: 100 mV/s.
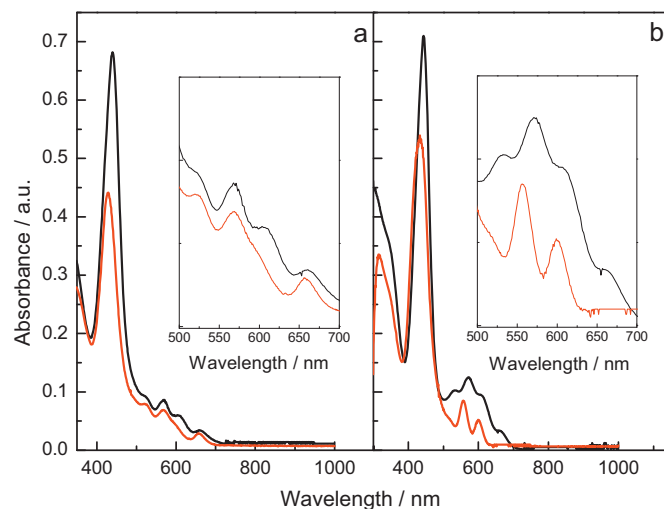

Fig. 8. Absorption spectra of electropolymerized bilayers (a) **A/B**, and (b) **B/A** on ITO electrodes. Red lines correspond to absorption of the first layers. Black lines correspond to absorption spectra of the complete bilayers films.

linear combination of the spectra of the component chromophores. Comparable spectra are observed after deposition of a first layer of **B** and a second one of **A** (Fig. 8b, red and black lines, respectively). The inset in Fig. 8b also shows the appearance of two new Q bands at around 539 and 660 nm, which are related to absorption of the **A** layer. It is well known that free base porphyrins present four Q bands (at about 500, 550, 600, and 650 nm), while the corresponding Zn derivatives present two Q bands at around 550 and 600 nm [33].

3.4. UV-Visible Absorption properties of electrodeposited C, A/C, and B/C bilayers

Fig. 9a and 9b show the absorption spectra of **C** in toluene solution and electrodeposited on ITO respectively. The last one presents two bands located at around 340 and 430 nm, and also a small broad band that extends from 580 to 1000 nm. The absorption spectra of the porphyrin polymer/**C** bilayers showed in Fig. 10 looked similar to the absorption spectra before deposition of the **C** layer, with the exception that a more defined band at around 340 nm appears. A contribution of the **C** layer is also observed for both bilayers in the zone between 580 to 1000 nm, which alters the shape of the Q
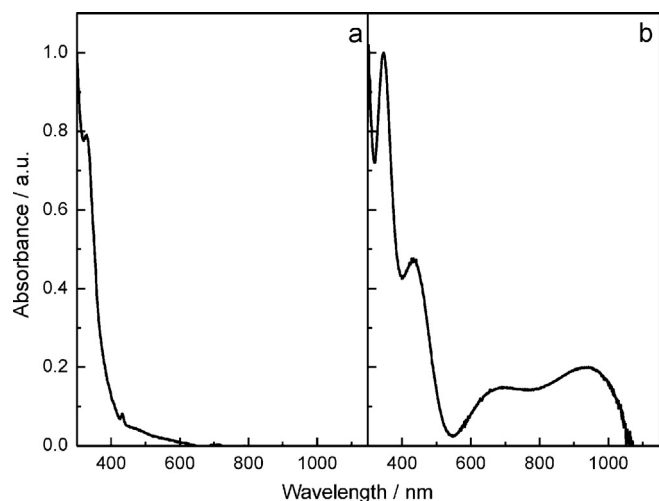

Fig. 9. Absorption spectra of (a) C in toluene solution, and (b) C electrodeposited film on ITO electrode.
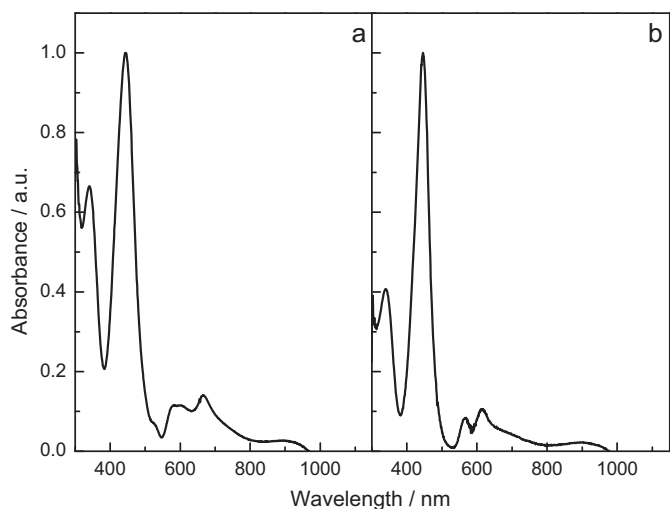
Fig. 10. Absorption spectra of electropolymerized films of (a) A/C, (b) B/C on ITO electrodes.

bands. The bands observed for **C** layer are attributed to absorption of the CBZ and C_{60} fulleropyrrolidine units [27,28,34,35].

3.5. Steady state and time resolved surface photovoltage spectroscopy of ITO/A/B and ITO/B/A double layer polymers

In order to analyze the effect of the configuration of polymer-polymer heterojuntions in the generation of photoinduced charge separation states, double layer polymers were prepared and SPV measurements were performed. **ITO/A/B** presents a photovoltage spectrum quite similar to the absorption spectrum, containing signals which correspond to both layers (Fig. 11a). However, contrarily to the SPV spectra observed for **ITO/A** single layer [21], the SPV sign of the in phase is negative, denoting that the electrons are separated preferentially towards the external surface (Fig. 11a). Also, the SPV value for this system is very low in comparison with **ITO/A** single layer polymer. This demonstrates that the presence of a second polymer layer of **B**, strongly affects the generation and
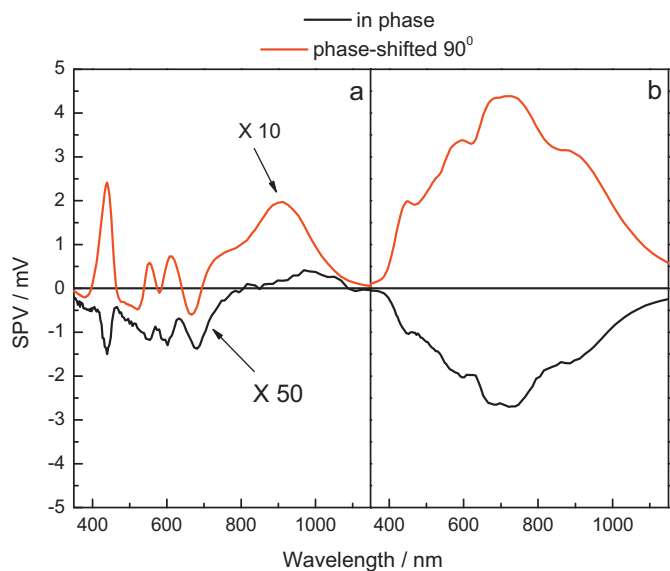

Fig. 11. SPV (surface photovoltage) spectra of electropolymerized bilayers (a) **A/B**, and (b) **B/A** on ITO electrodes. The experimental values in Fig. 11a are ten (phase-shifted 90^0) and fifty (in-phase) times enlarged.
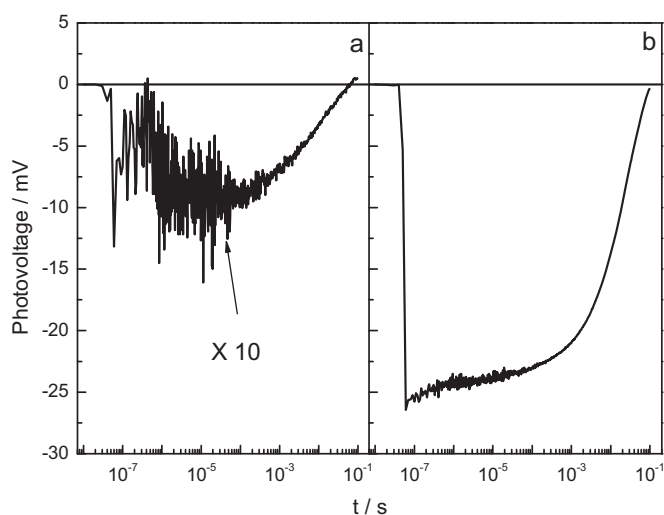

Fig. 12. Time resolved SPV signals of electropolymerized bilayers (a) **A/B**, and (b) **B/A** on ITO electrodes. $\lambda_{exc}=600$ nm.

recombination of the photoinduced charge carriers in **ITO/A/B** polymer system.

On the other hand, the SPV spectrum of **ITO/B/A** is also similar to the absorption spectrum of the double layer polymers, although the SPV signals are broadened in the 500-700 nm range (Fig. 11b). Besides, the illumination is also from the front side of the electrode, the high transmittance of the layers allows excitation of both polymers that form the bilayer. The SPV spectrum shows signals where both polymers present light absorption, indicating that both layers contribute to the generated photovoltage. **ITO/B/A** depicts a negative in-phase SPV signal (electrons separated towards the external surface), the same sign than that obtained for **ITO/B** single layer polymer. However the SPV amplitude for the bilayer is more than ten times higher than that observed for single layer polymers under similar experimental conditions [21].

The results show that porphyrin-porphyrin layers differ from the idealized donor-acceptor interface picture showed in Fig. 1. This could be due to the nature of the polymeric films which are not totally flat, and present a globular microstructure as a consequence of the nucleation and growing process, as we already reported [21]. Moreover, the ITO/polymers are also photoactive interfaces.

The high SPV value observed for **ITO/B/A** configuration could be explained taken into account that in **ITO/B** single layer electrons are separated towards the external surface of **B**, and holes travel to the ITO, after light absorption. Furthermore, it has been observed in different donor-acceptor systems formed by Zn and free base porphyrins that after light excitation energy and/or electron transfer occur, being the final state the charge separation state PZn$^{\cdot+}$-P$^{\cdot-}$, where P denotes a porphyrin residue [22–24,36]. Thus, when **A** is deposited on top of B (**ITO/B/A**), **A** acts as an electron acceptor for **B**, leaving the negative charge on the external surface of **A**. As a result of the movement of the electrons/holes the charge separation is increased.

In the case of **ITO/A/B** configuration, the observed photovoltage is much lower than in **ITO/A** films, as we already remarked, showing that the presence of **B** alters the performance of **A**. This could indicate a fast recombination of the photogenerated carriers, due to the presence of **B** in the outer layer, which is also seen in transient photovoltage experiments. Time resolved measurements (Fig. 12), showed that in both configurations (**ITO/A/B** and **ITO/B/A**) electrons are separated towards the external surface, but the SPV value for **ITO/A/B** is very low (Fig. 12a), contrarily to that observed for **ITO/A** film [21]. On the other hand, in the case of **ITO/B/A** the transient
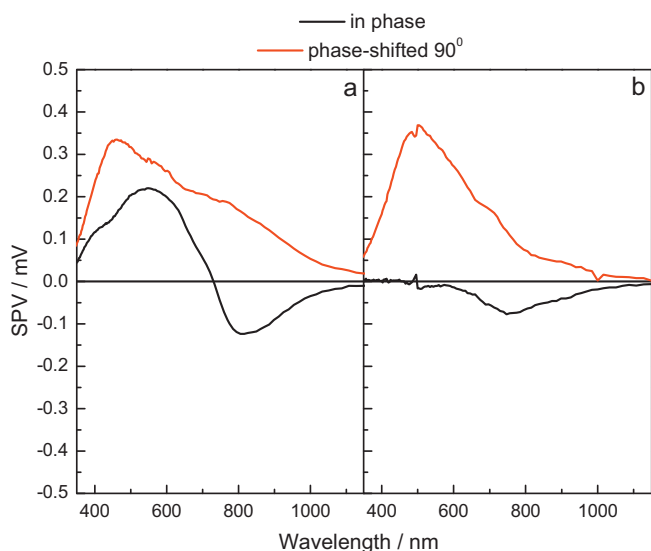
Fig. 13. SPV (surface photovoltage) spectra of electropolymerized bilayers (a) **A/C**, and (b) **B/C** on ITO electrodes.

Fig. 14. Time resolved SPV signals of electropolymerized bilayers (a) **A/C**, and (b) **B/C** on ITO electrodes. λ_{exc}=600 nm.

SPV is large(Fig. 12b), increasing within the laser pulse to around 25 times in comparison to **ITO/A/B** configuration. The charge separation state recombines slowly, and at around 10^{-2} sec the signal drops to half of the maximum value. These results clearly demonstrate that the electrochemical generated heterojunction in **ITO/B/A** configuration is the most efficient in the generation of photoinduced charge separation states in which **B** acts as a donor for **A**. It must be remarked that for a correct operation of donor-acceptor organic photovoltaic solar cells in most of the cases the donor is deposited on the ITO, and on top of the ITO/donor layer the acceptor layer is deposited.

3.6. Steady state and time resolved surface photovoltage spectroscopy of A/C, B/C, double layer polymers

The electrogenerated **A** and **B** films were modified by electrochemical deposition of a second layer of **C**, and SPV measurements were carried out. Fig. 13 shows the SPV spectra of the different double layer polymer configurations. **ITO/A/C** presents an in-phase SPV signal which changes from negative to positive, depending on the photon energy. In the range where **A** presents absorption the electrons are separated towards the internal surface, being this similar to the effect observed in **ITO/A** single layer [21]. This means that the presence of the electron acceptor outer C_{60} layer does not efficiently compensate the photoinduced charge separation attributed to **ITO/A** interface, which is opposite to the expected process for the **A/C** interface. This is corroborated by the transient photovoltage trace for **ITO/A/C** configuration which is quite similar to **ITO/A** film, where the excitation laser pulse at 600 nm is mainly absorbed by the porphyrin film (Fig. 14a). On the other hand for **ITO/B/C** the in-phase SPV signal is negative, indicating that the photogenerated electrons are separated towards the external surface, as it was observed for **ITO/B** single layer film. When **C** is present, the electrons located in the external surface of **B** can be accepted by **C**, leaving the negative charge on the C_{60}, external layer. However, the SPV amplitude values in both experiments do not show a marked increment, as we expected when a good electron acceptor as the C_{60} is present in the external layer. This could be due to the fact that electropolymerization of **C** does not form an idealized and thick film over the porphyrin layer. As it was mentioned electrodeposition of **C** could proceed by two ways. The first one may be the mechanism of dimerization of two **C** radical cations, and the
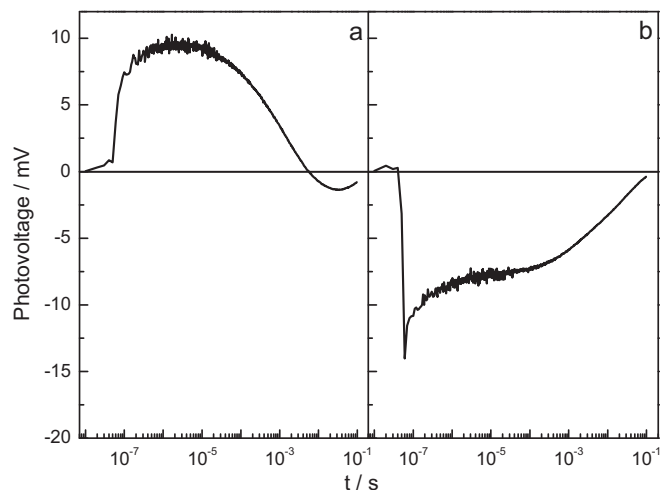
second one could probably be more complex, involving dimerization of free CBZ units present in the porphyrin layer with the CBZ units in the **C** solution, and/or both at the same time. These two mechanisms form a **C** layer on the globular structure of the porphyrin films, which does not efficiently contribute to an increase in the generation of photoinduced charge separation states.

4. Conclusions

The electrochemical formation of Zn(II) and free base porphyrin-porphyrin bilayers over ITO electrodes were performed by cyclic voltammetry using dicarbazole-diphenylamino functionalized dyes. Also a C_{60} derivative with carbazole moiety was synthesized and used in the generation of organic-organic heterojuntions. The electrochemical deposition of successive layers was corroborated by cyclic voltammetry and UV-visible absorption spectroscopy. Upon illumination ITO/Zn(II) porphyrin polymer/free-base porphyrin polymer (**ITO/B/A**) electrodes generate surface photovoltage amplitude more than ten times higher than that observed for single polymer layers, demonstrating that the electrochemical generated heterojunction **ITO/B/A** configuration is the most efficient in the generation of photoinduced charge separation states in which **B** acts as a donor for **A**. The results show that the electrochemical generated polymeric heterojunctions are able to produce photoinduced charge separated states, which present potential applications in the design and construction of organic optoelectronic devices. Contrarily, the electrochemical deposition of C_{60} electron acceptor did not show a noticeable effect on the generation of photoinduced charge separation states, measured by surface photovoltage. Improvements in the C_{60} electrochemical generated layer deposition method, based in new monomer functional structures, are under development.

References

[1] Z.B. Henson, K. Müllen, G.C. Bazan, Design strategies for organic semiconductors beyond the molecular formula, Nat. Chem. 4 (2012) 699.

[2] J. Wagner, M. Gruber, A. Hinderhofer, A. Wilke, B. Bröker, J. Frisch, P. Amsalem, A. Vollmer, A. Opitz, N. Koch, F. Schreiber, W. Brütting, High fill factor and open circuit voltage in organic photovoltaic cells with diindenoperylene as donor material, Adv. Funct. Mater. 20 (2010) 4295.

[3] M. Gervaldo, M. Funes, J. Durantini, L. Fernandez, F. Fungo, L. Otero, Electrochemical polymerization of palladium (II) and free base 5,10,15,20-tetrakis(4-N,N-diphenylaminophenyl)porphyrins: Its applications as electrochromic and photoelectric materials, Electrochim. Acta 55 (2010) 1948.

[4] B. Lu, J. Yan, J. Xu, S. Zhou, X. Hu, Novel electroactive proton-doped conducting poly(aromatic ethers) with good fluorescence properties via electropolymerization, Macromolecules 43 (2010) 4599.

[5] P.A. Liddell, M. Gervaldo, J.W. Bridgewater, A.E. Keirstead, S. Lin, T.A. Moore, A.L. Moore, D. Gust, Porphyrin-based hole conducting electropolymer, Chem. Mater. 20 (2008) 135.

[6] L. Xu, J. Zhao, C. Cui, R. Liu, J. Liu, H. Wang, Electrosynthesis and characterization of an electrochromic material from poly(1,4-bis(2-thienyl)-benzene) and its application in electrochromic devices, Electrochim. Acta 56 (2011) 2815.

[7] M. Li, S. Tang, F. Shen, M. Liu, F. Li, P. Lu, D. Lu, M. Hanif, Y. Ma, The counter anionic size effects on electrochemical, morphological, and luminescence properties of electrochemically deposited luminescent films, J. Electrochem. Soc. 155 (2008) H287–H291.

[8] E. Nasybulin, J. Feinstein, M. Cox, I. Kymissis, K. Levon, Electrochemically prepared polymer solar cell by three-layer deposition of poly(3,4-ethylenedioxythiophene)/poly(2,20-bithiophene)/fullerene (PEDOT/PBT/C_{60}), Polymer 52 (2011) 3627.

[9] E. Nasybulin, M. Cox, I. Kymissis, K. Levon, Electrochemical codeposition of poly(thieno[3,2-b]thiophene) and fullerene: An approach to a bulk heterojunction organic photovoltaic device, Synth. Met 162 (2012) 10.

[10] C.-Y. Lin Lo, C.-F. Luo, H.-P. Lu, C.-S. Hung, E.W.-G. Diau, Design and characterization of novel porphyrins with oligo(phenylethylnyl) links of varied length for dye-sensitized solar cells: synthesis and optical, electrochemical, and photovoltaic investigation, J. Phys. Chem. C 113 (2009) 755.

[11] K. Takahashi, I. Nakajima, K. Imoto, T. Yamaguchia, T. Komura, K. Murata, Sensitization effect by porphyrin in polythiophene/perylene dye two-layer solar cells, Sol. Energy Mater. Sol. Cells 76 (2003) 115.

[12] J. Chen, A.K. Burrell, W.M. Campbell, D.L. Officer, C.O. Too, G.G. Wallace, Photoelectrochemical cells based on a novel porphyrin containing light harvesting conducting copolymer, Electrochim. Acta 49 (2004) 329.

[13] K. Miyairi, E. Itoh, Y. Hashimoto, Photovoltaic properties of double layer devices consisting of titanium dioxide and porphyrin dispersed hole transporting material layer, Thin Solid Films 438 (2003) 147.

[14] F. D'Souza, O. Ito, Photosensitized electron transfer processes of nanocarbons applicable to solar cells, Chem. Soc. Rev. 41 (2012) 86.

[15] D. Wróbel, Organic photovoltaic solar cells: spectroscopic and photoelectric properties of photoactive dyes, Comptes Rendus Chimie 6 (2003) 417.

[16] D. Wróbel, A. Boguta, A. Wójcik, R.M. Ion, Time-resolved photocurrent generation in a photoelectrochemical cell with phthalocyanine, Spectrochim. Acta 61 (2005) 1127.

[17] K. Takechi, T. Shiga, T. Motohiro, T. Akiyama, S. Yamada, H. Nakayama, K. Kohama, Solar cells using iodine-doped polythiophene–porphyrin polymer films, Sol. Energy Mater. Sol. Cells 90 (2006) 1322.

[18] M. Schäferling, P. Bäuerle, Porphyrin-functionalized oligo- and polythiophenes, J. Mater. Chem. 14 (2004) 1132.

[19] E.T. Seo, R.F. Nelson, J.M. Fritsch, L.S. Marcoux, D.W. Leedy, R.N. Adams, Anodic oxidation pathways of aromatic amines. Electrochemical and electron paramagnetic resonance studies, J. Am. Chem. Soc. 88 (1966) 3498.

[20] S.N. Kuester, M.M. McGuire, S.M. Drew, Electrochemically initiated polymerization of zinc(II)5-vinyl-10,15,20-triphenylporphyrin, J. Electroanal. Chem 452 (1998) 13.

[21] J. Durantini, G.M. Morales, M. Santo, M. Funes, E.N. Durantini, F. Fungo, Th. Dittrich, L. Otero, M. Gervaldo, Synthesis and characterization of porphyrin electrochromic and photovoltaic electropolymers, Org. Electron. 13 (2012) 604–614.

[22] F. Fungo, L. Otero, E.N. Durantini, J.J. Silber, L. Sereno, Photosensitization of thin SnO_2 nanocrystalline semiconductor film electrodes with metallodiporphyrin, J. Phys. Chem B 104 (2000) 7644.

[23] D. Gust, T.A. Moore, A.L. Moore, L. Leggett, S. Lin, J.M. DeGraziano, R.M. Hermant, D. Nicodem, P. Craig, G.R. Seely, R.A. Nieman, Photoinduced electron transfer in a porphyrin dyad, J. Phys. Chem. 97 (1993) 7926.

[24] D. Gust, T.A. Moore, A.L. Moore, H.K. Kang, J.M. DeGraziano, P.A. Liddell, G.R. Seele, Effect of coordinated ligands on interporphyrin photoinduced-electron-transfer rates, J. Phys. Chem. 97 (1993) 13637.

[25] H. Imahori, S. Fukuzumi, Porphyrin-and fullerene-based molecular photovoltaic devices, Adv. Funct. Mater. 14 (2004) 525.

[26] Th. Dittrich, S. Bönisch, P. Zabel, S. Dube, High precision differential measurement of surface photovoltage transients on ultrathin CdS layers, Rev. Sci. Instrum. 79 (2008) 113903 (1-6).

[27] U.K. Hee, M. Dongbo, K. Ji-Hoon, B.P. Jong, C.Y. Sung, C.Y. Ung, H. Do-Hoon, Carbazole-containing fullerene derivatives for P3HT-based bulk-heterojunction solar cells, Sol. Energy Mater. Sol. Cells 105 (2012) 6.

[28] M. Dongbo, K. Ji-Hoon, C.Y. Sung, L. Changjin, L. Jin-Kyun, H. Do-Hoon, Synthesis and characterization of a novel fullerene derivative containing carbazole group for use in organic solar cells, Synth. Met. 161 (2011) 1330.

[29] J.F. Ambrose, R.F. Nelson, Anodic oxidation pathways of carbazoles: I. carbazole and n-substituted derivatives, J. Electrochem. Soc. 115 (1968) 1159.

[30] L. Echegoyen, L.E. Echegoyen, Electrochemistry of fullerenes and their derivatives, Acc. Chem. Res. 31 (1998) 593.

[31] J.F. Ambrose, L.L. Carpenter, R.F. Nelson, Electrochemical and spectroscopic properties of cation radicals iii. reaction pathways of carbazolium radical ions, J. Electrochem. Soc. Electrochem. Sci. Technol. 122 (1975) 876.

[32] C. Bruno, M. Marcaccio, D. Paolucci, C. Castellarin-Cudia, A. Goldoni, A.V. Streletskii, T. Drewello, S. Barison, A. Venturini, F. Zerbetto, F. Paolucci, Growth of p- and n-dopable films from electrochemically generated C60 cations, J. Am. Chem. Soc. 130 (2008) 3788.

[33] C.-W. Huang, K.Y. Chiu, S.-H. Cheng, Novel spectral and electrochemical characteristics of triphenylamine-bound zinc porphyrins and their intramolecular energy and electron transfer, Dalton Trans. 14 (2005) 2417.

[34] M. Lapkowski, J. Zak, K. Karon, B. Marciniec, W. Prukala, The mixed carbon–nitrogen conjugation in the carbazole based polymer; the electrochemical, UV-Vis, EPR, and IR studies on 1,4 bis[(E)2-(9H-carbazol-9-yl)vinyl]benzene, Electrochim. Acta 56 (2011) 4105.

[35] X. Ouyanga, G. Zengc, H. Zenga, W. Ji, Synthesis, third-order nonlinear absorption and refraction of fullerene dyads containing fluorine, J, Photochem. Photobiol. A: Chem. 213 (2010) 7.

[36] M. Gervaldo, L. Otero, M.E. Milanesio, E.N. Durantini, J.J. Silber, L.E. Sereno, Photosensitization of thin SnO_2 nanocrystalline semiconductor film electrodes with electron donor–acceptor metallodiporphyrin dyad, Chemical Physics 312 (2005) 97.